Available online at www.sciencedirect.com
SCIENCE DIRECT®
Biochemical Pharmacology 68 (2004) 2263–2271
Biochemical Pharmacology
www.elsevier.com/locate/biochempharm

Influence of phenylalanine 120 on cytochrome P450 2D6 catalytic selectivity and regiospecificity: crucial role in 7-methoxy-4-(aminomethyl)-coumarin metabolism

Peter H.J. Keizers, Barbara M.A. Lussenburg, Chris de Graaf, Letty M. Mentink, Nico P.E. Vermeulen, Jan N.M. Commandeur*

LACDR/Division of Molecular Toxicology, Department of Pharmacochemistry, Vrije Universiteit, De Boelelaan 1083, 1081 HV Amsterdam, The Netherlands

Received 17 May 2004; accepted 2 August 2004

Abstract

The polymorphic human debrisoquine hydroxylase, cytochrome P450 2D6 (CYP2D6), is one of the most important phase I drug metabolising enzymes. It is responsible for metabolising a large number of compounds that mostly share similarity in having a basic N-atom and an aromatic moiety. In homology modelling studies, it has been suggested that in fixation of this aromatic moiety, there may be an important role for phenylalanine 120 (Phe^{120}). In this study, the role of Phe^{120} in ligand binding and catalysis was experimentally examined by mutating it into an alanine. Strikingly, this substitution led to a completely abolished 7-methoxy-4-(aminomethyl)-coumarin (MAMC) *O*-demethylating activity of CYP2D6. On the other hand, bufuralol metabolism was hardly affected (K_m of 1-hydroxylation mutant: 1.2 μM, wild-type: 2.9 μM, 4-hydroxylation mutant: 1.5 μM, and wild-type: 3.2 μM) and neither was affected dextromethorphan *O*-demethylation (K_m mutant: 1.2 μM, wild-type: 2 μM, k_{cat} mutant: 4.5 min^{-1}, and wild-type: 3.3 min^{-1}). However, the Phe^{120}Ala mutant also formed 3-hydroxymorphinan, the double demethylated form of dextromethorphan, which was not detected using wild-type CYP2D6. 3,4-Methylenedioxymethamphetamine (MDMA) was demethylenated by both mutant and wild-type CYP2D6 to 3,4-dihydroxymethamphetamine (3,4-OH-MA K_m of mutant: 55 μM and wild-type: 2 μM). In addition, the mutant formed two additional metabolites; 3,4-methylenedioxyamphetamine (MDA) and *N*-hydroxy-3,4-methylenedioxymethamphetamine (*N*-OH-MDMA). Inhibition experiments of dextromethorphan *O*-demethylation showed a decreased affinity of the Phe^{120}Ala mutant for quinidine (IC_{50} mutant: 240 nM and wild-type, 40 nM), while IC_{50}s for quinine were equal (1 μM). These data indicate the importance of Phe^{120} in the selectivity and regiospecificity in substrate binding and catalysis by CYP2D6.

Keywords: Cytochrome P450 2D6; MDMA; MAMC; Mutagenesis; *N*-Demethylation; *N*-Hydroxylation

1. Introduction

Cytochromes P450 (CYPs) are heme-containing enzymes capable of oxidizing and reducing a large variety of endogenous and exogenous substrates in virtually all living organisms [1,2]. In humans, one of the most important hepatic phase I drug metabolising enzymes is CYP2D6. It is involved in the metabolism of about 30% of the currently marketed drugs, including neuroleptics, antidepressants β-blockers, opioids and antiarythmics [3,4]. The enzyme is known for its genetic polymorphisms, even increasing its clinical relevance [5,6]. Although some crystal structures of mammalian CYPs have become available in recent years [7,8], so far no crystal structure of CYP2D6 has been resolved. Structural information on this enzyme still depends on homology modelling and mutagenesis studies.

Recently we have developed a new homology model of CYP2D6 based on the crystal structure of rabbit CYP2C5 [9]. This was the first model of CYP2D6 based on a

Abbreviations: CYP, cytochrome P450; MAMC, 7-methoxy-4-(aminomethyl)-coumarin; Phe^{120}Ala, phenylalanine 120 → alanine; MDMA, 3,4-methylenedioxymethylamphetamine; 3,4-OH-MA, 3,4-dihydroxymethamphetamine; MDA, 3,4-methylenedioxyamphetamine; *N*-OH-MDMA, *N*-hydroxy-3,4-dihydroxymethylamphetamine; HAMC, 7-hydroxy-4-(aminomethyl)-coumarin; AU, arbitrary units; T_r, retention time

* Corresponding author. Tel.: +31 20 444 7595; fax: +31 20 444 7610.
E-mail address: command@few.vu.nl (Jan N.M. Commandeur).

0006-2952/$ – see front matter © 2004 Elsevier Inc. All rights reserved.
doi:10.1016/j.bcp.2004.08.013

mammalian CYP template and is therefore considered an improvement over the existing models. This was indicated by the good correlation between experimental data and the modelled protein–substrate interactions. The model identified some active site key residues. First of all, Glu^{216} has been shown to be a key ligand-binding residue involved in hydrogen bonding with a variety of substrates. This residue has been subjected to several mutagenesis studies [10,11] that indicated involvement of this residue in fixation of basic nitrogen atoms present in many CYP2D6 substrates. A second important active site residue in this and in other homology models is Phe^{483} [12], interacting via van der Waals forces with substrates like codeine. Earlier mutagenesis of this residue to an isoleucine showed effects on testosterone metabolism [13]. However, the anchoring of aromatic moieties present in most CYP2D6 substrates, as predicted in pharmacophore models [14–16], cannot be completely ascribed to this residue. Therefore, other Phe residues contributing to aromatic interactions with substrates have to be present in the active site. Mutation of Phe^{481} to other non-aromatic residues led to decreased activities towards model substrates [17], although in the model of Venhorst et al., this residue is not considered to be in the active site of CYP2D6.

Even more interesting is the position of a third phenylalanine at position 120 in the active site of CYP2D6 homology models [9,11,12]. In these CYP2C5-based models Phe^{120} appears to be positioned directly above the porphyrin ring. From docking and molecular dynamics studies, this residue seems to be the anchoring residue for the aromatic moiety of ligands like quinidine and sparteine via π–π stacking [9]. In the present study, the role of Phe^{120} in ligand binding and metabolism by CYP2D6 is studied experimentally by mutating this residue into an alanine. According to computational simulations, this mutation will not only create more space in the active site, but also eliminate a potentially important aromatic anchoring point. By mutating Phe^{120} into Ala, we are aiming at the elucidation of the role of this residue in substrate binding and turnover by CYP2D6.

2. Materials and methods

2.1. Materials

The pSP19T7LT_2D6 plasmid containing human 2D6 with a C-terminal His_6-tag bicistronically co-expressed with human cytochrome P450 NADPH reductase was kindly provided by Prof. Dr. Ingelman-Sundberg. 7-Methoxy-4-(aminomethyl)-coumarin (MAMC), 7-hydroxy-4-(aminomethyl)-coumarin (HAMC), 3,4-methylenedioxymethylamphetamine (MDMA) and 3,4-methylenedioxyamphetamine (MDA) were synthesised as described [18,19]. Bufuralol hydrochloride was obtained from Gentest. *N*-Methylhydroxylamine hydrochloride, dextromethorphan hydrobromide and dextrorphan tartrate were obtained from Sigma. All other chemicals were of analytical grade and obtained from standard suppliers.

2.2. Synthesis of N-hydroxy-3,4-dihydroxymethylamphetamine

N-Hydroxy-3,4-dihydroxymethylamphetamine (1-(3,4-methylenedioxyphenyl)-*N*-methyl,2-hydroxylaminopropane) was prepared from piperonyl methyl ketone and *N*-methylhydroxylamine by reductive amination with sodium cyanoborohydride [20]. A two-fold surplus of *N*-methylhydroxylamine hydrochloride was stirred with piperonyl methyl ketone in methanol at room temperature and then sodium cyanoborohydride was added and stirred for additional 48 h. After adding water, neutralising the cyanoborohydride with 6 M HCl and neutralising the acid with 6 M NaOH, the product was extracted in dichloromethane.

^{1}H NMR (400 Hz, $CDCl_3$): δ 1.00 (d, 3H, CCH_3), 2.38 (dd, 1H, H-1), 2.68 (s, 3H, NCH_3), 2.91 (m, 1H, CHN), 3.10 (dd, 1H, H-1), 5.90 (s, 2H, OCH_2O), 6.63 (dd, 1H, H-6′), 6.70 (d, 1H, H-2′), and 6.72 (d, 1H, H-5′). ^{13}C NMR (400 Hz, $CDCl_3$): δ 14.20 (CH_3), 38.82 (CH_2), 43.95 (CH_3N), 65.35 (CH), 72.82, 100.83 (OCH_2O), 108.17 (C-5′), 109.70 (C-2′), 122.13 (C-6′), 133.29 (C-1′), 145.87 (C-4′), and 147.59 (C-3′). MS direct injection: *m/z*, $M^{\bullet+}$ 210, and MS/MS: 179 (3), 163 (100), and 135 (3).

2.3. Site-directed mutagenesis

The phenylalanine 120 → alanine ($Phe^{120}Ala$) mutation was introduced into pSP19T7LT_2D6 using the QuickChange XL site-directed mutagenesis kit (Stratagene). The sequences of the forward- and reverse-oligonucleotides, respectively, with the mutated residue in italic, were as follows: 5′-CGT TCC CAA GGG GTG *GCC* CTG GCG CGC TAT-3′ and 5′-ATA GCG CGC CAG *GGC* CAC CCC TTG GGA ACG-3′. After mutagenesis, the presence of the desired $Phe^{120}Ala$ mutation was confirmed by DNA sequencing.

2.4. Expression and membrane isolation

Both the $Phe^{120}Ala$ mutant and the wild-type pSP19T7LT_2D6 plasmids were transformed into *Escherichia coli* strain JM109. Expression was carried out in 3 l flasks containing 300 ml Terrific Broth (TB) medium with additives (1 mM δ-aminolevulinic acid, 400 μl/l trace elements [21], 1 μg/ml thiamine, and 100 μg/ml ampicillin). Cultures were inoculated with 3 ml of frozen *E. coli* cells containing the desired plasmid and induction was initiated by the addition of 2 mM isopropyl β-D-thiogalactoside. Cultures were grown for 48 h at 28 °C and 125 rpm, before they were harvested. CYP contents were determined by CO difference spectra [22].

Harvested cells were pelleted by centrifugation (15 min, 4000 × *g*, and 4 °C) and the resulting pellet was resuspended in TSE buffer (50 mM tris–acetate pH 7.6, 250 mM sucrose, and 0.25 mM EDTA) to 35 mg wet weight cells/ml. Spheroblasts were prepared by adding 0.1 mg/ml lysozyme and gently shaking the cells for 30 min on ice. Spheroblasts were pelleted by centrifugation (15 min, 4000 × *g*, and 4 °C) and resuspended in KPi–glycerol buffer (100 mM potassium phosphate buffer, pH 7.4, 20% glycerol and 0.1 mM DTT) to 0.5 g/ml. The spheroblasts were lysed by passage through a French press followed by sonication (Branson Sonifier 250, 10 × 20 s, at 70% full power) and the membrane fraction was isolated by ultracentrifugation (45 min, 120,000 × *g*, and 4 °C). Membranes were resuspended in 0.4% of the original culture volume of TSE buffer and CYP contents were determined with CO difference spectra.

2.5. Metabolism and inhibition assays

MAMC *O*-demethylation [23]: reactions were carried out in duplicate in a 96-wells plate, in a total volume of 200 μl. The reaction mixture consisted of 50 mM potassium phosphate buffer (KPi) pH 7.4, 5 mM $MgCl_2$, 0–500 μM MAMC (10 concentrations used) and *E. coli* membranes (40 nM wild-type or $Phe^{120}Ala$ mutant CYP2D6). The reactions were initiated by addition of an NADPH regenerating system, resulting in final concentrations of 0.1 mM NADPH, 0.3 mM glucose-6-phosphate, 1 mM $MgCl_2$ and 0.4 units/ml glucose-6-phosphate dehydrogenase. The reaction was monitored for 40 min at 37 °C on a Victor^2 1420 multilabel counter (Wallac) (λ_{ex} = 405 nm and λ_{em} = 460 nm). The metabolite of MAMC, i.e. HAMC, was identified and quantified using the synthetic reference compound. HPLC analysis of MAMC metabolism was performed as described [18], using a C18 column (Chrompack Chromspher 5 and 250 mm × 4.6 mm) with a flow rate of 0.4 ml/min.

Dextromethorphan *O*-demethylation [10]: reactions were carried out in 300 μl of 50 mM KPi pH 7.4, 5 mM $MgCl_2$ supplemented with 10 concentrations ranging from 0 to 40 μM dextromethorphan and *E. coli* membranes (50 nM wild-type or 25 nM $Phe^{120}Ala$ mutant CYP2D6). After 5 min of pre-incubation at 37 °C, the reactions were initiated with an NADPH regenerating system as described above. The reaction was allowed to proceed for 5 min before it was stopped by the addition of 15 μl of 70% $HClO_4$. After centrifugation (10 min at 6800 × *g*), 30-μl aliquots of the supernatant were analysed by HPLC. Metabolites were separated using a C18 column (Chrompack Chromspher 5 and 250 mm × 4.6 mm) with a flow rate of 1 ml/min. The mobile phase consisted of 30% acetonitrile and 1% triethylamine, set to pH 3 with 70% $HClO_4$. Metabolites were detected by fluorescence (λ_{ex} = 280 nm and λ_{em} = 311 nm) and identified by LC–MS. Inhibition of *O*-demethylation by various concentrations of quinidine and quinine was measured under the same conditions using a concentration of 8 μM dextromethorphan.

Bufuralol hydroxylation [10,24]: reactions were carried out as described above with nine concentrations ranging from 0 to 100 μM bufuralol and *E. coli* membranes (50 nM wild-type or 25 nM $Phe^{120}Ala$ mutant CYP2D6). Metabolites were separated using a C18 column (Chrompack Chromspher 5, dimensions: 250 mm × 4.6 mm) with a flow rate of 0.6 ml/min. The mobile phase consisted of 30% acetonitril and 0.1% triethylamine, set to pH 3 with 70% $HClO_4$. Metabolites were detected by fluorescence (λ_{ex} = 252 nm and λ_{em} = 302 nm). Metabolites of bufuralol were identified by comparison with other studies [24].

MDMA metabolism: reactions were carried out as described above with nine concentrations ranging from 0 to 200 μM MDMA and *E. coli* membranes (50 nM wild-type or 25 nM $Phe^{120}Ala$ mutant CYP2D6). Metabolites were separated using a C18 column (Phenomenex Inertsil ODS, dimensions: 150 mm × 4.6 mm) with a flow rate of 0.4 ml/min. The mobile phase consisted of 23% acetonitrile and 0.1% triethylamine, set to pH 3 with 70% $HClO_4$. Metabolites were detected by fluorescence (λ_{ex} = 280 nm and λ_{em} = 320 nm), electrochemical detection (ECD, oxidation mode 0.8 V for detection of 3,4-OH-MA), LC–MS (3,4-OH-MA, MDA, *N*-OH-MDMA) and by synthesised reference compounds (MDA, *N*-OH-MDMA).

Peak areas of all metabolites were quantified by Shimadzu class VP 4.3 and analysed using Graph Pad Prism 4.0.

2.6. LC–MS

To identify the metabolites of MDMA, dextromethorphan and dextrorphan, incubations were carried out for 10 min as described above with 100 μM MDMA, 100 μM dextrorphan or 25 μM dextromethorphan, respectively, and *E. coli* membranes (50 nM 2D6 wild-type or 50 nM 2D6 $Phe^{120}Ala$). Volumes of 100 μl supernatant were injected and separated using a phenyl column (Waters Novapak phenyl, dimensions: 150 mm × 4.6 mm) with a flow rate of 0.4 ml/min. The metabolites were eluted using a gradient starting with a 1% ACN eluens, supplemented with 10 mM ammonium acetate, increasing linearly to 95% ACN with 10 mM ammoniumacetate in 30 min and analysed by MS. APCI-positive ionisation was used on a LCQ Deca mass spectrometer (Thermo Finnigan), vaporizer temperature 450 °C, N_2 as sheath (40 psi), auxiliary gas (10 psi), needle voltage 6000 V, and heated capillary at 150 °C.

2.7. Homology modelling

A protein homology model of CYP2D6 was constructed based on the crystal structures of dimethylsulphophenazole and diclofenac bound rabbit CYP2C5, PDB codes 1N6B and 1NR6, respectively [7,25]. Homology modelling,

model refinement and model validation were performed as described [9]. The final model of wild-type CYP2D6 was used as a template for modelling of the Phe^{120}Ala mutant. The Phe^{120} residue was mutated to Ala using the homology module of InsightII (Biosym), after which an energy minimisation and a 1 ps position re-strained molecular dynamics simulation was carried out.

3. Results

3.1. Expression of wild-type and Phe^{120}Ala mutant CYP2D6

The Phe^{120}Ala mutant had consistently significantly lower expression levels compared to wild-type CYP2D6. An average culture contained about 70 nM of CYP for the mutant versus 200 nM for wild-type after 48 h induction. In the difference spectrum taken from the culture of the mutant enzyme, a high absorbance was measured at 420 nm showing the presence of large amounts of P420, the inactive form of CYP, indicating that the mutation decreases the stability of the enzyme to some extent.

3.2. Metabolism of model compounds

O-Demethylation of the CYP2D6 marker substrate MAMC (Fig. 1) showed to be linear for over 40 min using *E. coli* membranes containing 40 nM of wild-type CYP2D6. Enzyme kinetics analysis revealed a K_m of 49 μM and a k_{cat} of 3.7 min^{-1} (Table 1). Using the Phe^{120}Ala mutant under the same conditions did not lead to detectable HAMC formation. HPLC analysis of these incubations gave the same results and did not show any additional metabolites.

Dextromethorphan was selectively *O*-demethylated to dextrorphan by wild-type CYP2D6 (K_m = 2 μM and k_{cat} = 3.3 min^{-1}). The Phe^{120}Ala mutant also formed dextrorphan be it with a slightly lower K_m and higher k_{cat} than the wild-type. The formation of dextrorphan showed to be linear for at least 20 min, indicating the mutant to be stable enough for studying the metabolism. Dextrorphan and other metabolites were identified by LC–MS. The *N*-demethylated metabolite of dextromethorphan, i.e. 3-methoxymorphinan (*m/z* 258 and MS/MS: *m/z* 215) was detected for both the wild-type as for the Phe^{120}Ala mutant with a T_r of 36 min. Because of overlap with the peak of dextromethorphan (*m/z* 272 and MS/MS: *m/z* 215) at T_r of 37 min, *N*-demethylation could not be quantified. Interestingly, also a metabolite with *m/z* 244 (T_r = 31.1 min and MS/MS: *m/z* 147) was detected for the Phe^{120}Ala mutant, apparently the double *O*- and *N*-demethylated metabolite of dextromethorphan, i.e. 3-hydroxymorphinan. The 3-hydroxymorphinan formation could also not be quantified under the conditions used because it is a secondary metabolite. When the Phe^{120}Ala mutant was incubated with dextrorphan again 3-hydroxymorphinan was formed and two other metabolites with *m/z* 274 were detected (T_r = 27.5 min, MS/MS: *m/z* 199 and T_r = 30.3 min MS/MS: *m/z* 257 and 201), indicating hydroxylation of dextrorphan. With the wild-type CYP2D6, no metabolites of dextrorphan were detected.

Upon incubation of bufuralol both with wild-type and Phe^{120}Ala mutant CYP2D6, four metabolites were detected; 6-OH bufuralol, 1′-OH bufuralol, 4-OH bufuralol and $\Delta^{1',2'}$ bufuralol, as identified before by others [24]. Under the conditions used, only peak areas of the metabolites 1′-OH bufuralol and 4-OH bufuralol could be quantified. For both these metabolites the Phe^{120}Ala mutant showed a two times lower K_m than wild-type CYP2D6 with a comparable turnover (Table 1).

Another known CYP2D6 substrate that was subjected to incubations with wild-type and Phe^{120}Ala mutant CYP2D6 was MDMA [26]. In the case of wild-type CYP2D6, only demethylenenation of MDMA to the catechol 3,4-dihydroxymethylamphetamine (3,4-OH-MA) was observed with a K_m of 2 μM and a V_{max} of 3.4 × 10^5 AU. This metabolite was identified by ECD, LC–MS (measured as the quinone, T_r 21.2 min, and *m/z* 180) and it was described before by others [26]. The mutant enzyme also formed this catechol with a similar V_{max}, but with a 30-fold higher K_m (Fig. 2). In addition to demethylenenation, MDMA was also *N*-demethylated to MDA by the mutant enzyme with a K_m of 9 μM and a V_{max} of 6 × 10^5 AU, as identified by LC–MS (T_r = 21.4 min and *m/z* 180) and co-elution with the synthetic reference (Fig. 2). Furthermore, a third metabolite was formed by the Phe^{120}Ala mutant with a K_m of 11 μM and a V_{max} of 11 × 10^5 AU. This metabolite was also identified by LC–MS. A *m/z* of 210 was observed for this metabolite (T_r = 21.9 min), indicating hydroxylation of MDMA (*m/z* 194). MS/MS data showed a mass over charge of 163, suggesting that hydroxylation took place on the nitrogen, as the *m/z* of 163 is the propyl-methylenedioxyphenyl fragment, which is also a common fragment of both MDA and MDMA. In order to confirm the identity of this new metabolite of MDMA, *N*-OH-MDMA was synthesised and showed identical mass spectroscopic behaviour. Direct injection of this compound in the MS gave a *m/z* 210, with as the major MS/MS fragment *m/z* 163. In addition, the *N*-OH-MDMA also co-eluted with the new metabolite on both the C18 as the phenyl reversed phase columns, when spiked in an incubation sample, verifying it to have the same molecular structure.

3.3. Inhibition of dextromethorphan metabolism

Inhibition of dextromethorphan *O*-demethylation by quinidine and quinine was determined for both Phe^{120}Ala and wild-type CYP2D6 (Fig. 3). In case of both the enzymes quinine inhibited dextrorphan formation with an IC_{50} of about 1 μM (Table 2), whereas quinidine was about six-fold less potent in inhibiting the Phe^{120}Ala

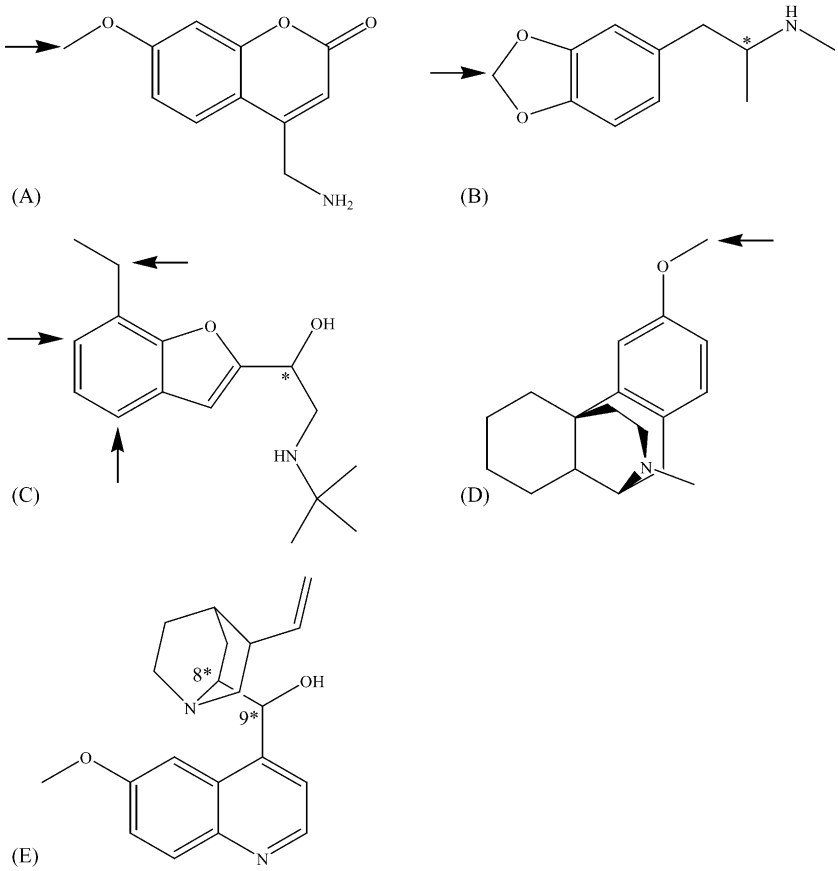

Fig. 1. Structures of the substrates (A: MAMC, B: MDMA, C: bufuralol, D: dextromethorphan) and ligands (E: quinidine (8R, 9S) and quinine (8*S*, 9*R*)) used, showing sites of oxidation by wild-type CYP2D6 (↑) and chiral carbon atoms (*).

mutant (IC_{50} 200 nM) than the wild-type enzyme (IC_{50} 40 nM).

3.4. Modelling

In a refined homology model of CYP2D6 used in this study; Phe^{120}, Glu^{216}, and Phe^{483} are positioned at approximately the same location as in the previously reported homology model [9]. Asp^{301}, however, does not point into the active site, but is oriented such that it stabilises the B/C-loop by hydrogen bonding to the backbone N-atoms of residues Val^{119} and Phe^{120}. Asp^{301}, however, may also play an electrostatic role in the binding of basic substrates by increasing the net negative charge within the active site

Table 1
Metabolism of model compounds by wild-type and Phe^{120}Ala mutant CYP2D6

Compound	Metabolites	Wild-type		Phe^{120}Ala	
		K_m	V_{max}	K_m	V_{max}
MAMC	HAMC	49 ± 2	3.7 ± 0.6[a]	–[b]	–[b]
Dextromethorphan	Dextrorphan	2.0 ± 0.2	3.3 ± 0.4[a]	1.2 ± 0.4	4.5 ± 0.3[a]
	3-OH-morphinan	–[b]	–[b]	+[c]	+[c]
Dextrorphan	3-OH-morphinan	–[b]	–[b]	+[c]	+[c]
Bufuralol	1′-OH	2.9 ± 0.4	54 ± 17[d]	1.2 ± 0.2	51 ± 11[d]
	4-OH	3.2 ± 0.5	2.7 ± 0.8[d]	1.5 ± 0.3	2.7 ± 0.6[d]
MDMA	3,4-OH-MA	1.9 ± 0.7	3.4 ± 1.0[d]	55.4 ± 16	4.6 ± 1.1[d]
	MDA	–[b]	–[b]	9.0 ± 2.5	6.0 ± 3.3[d]
	N-OH-MDMA	–[b]	–[b]	11.0 ± 2.8	10.9 ± 3.8[d]

All values are the means of at least three independent experiments ± S.D. as described in Section 2.5. K_m expressed in μM.
[a] V_{max} expressed in min^{-1}.
[b] Not detectable.
[c] Present but not quantifiable.
[d] V_{max} expressed in 1×10^5 fluorescence units/(min nmol) P450.

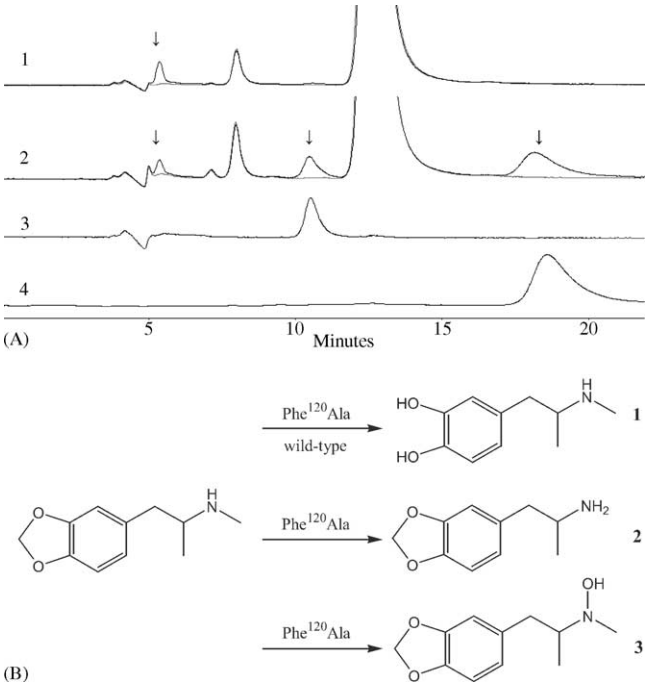

Fig. 2. Chromatograms of 100 μM MDMA incubations with membranes of *E. coli* cells expressing wild-type (1) and Phe^{120}Ala mutant (2) CYP2D6 with (gray) and without (black) 20 μM quinidine are shown in (A). Metabolites are indicated (↓) and reference chromatograms of synthesised MDA (3) and synthesised *N*-OH-MDMA (4) are also shown. T_r of the substrate MDMA is 13.2 min, T_r of metabolites: 3,4-OH-MA 5.5 min, MDA 10.9 min, and *N*-OH-MDMA 18.8 min. For conditions used see Section 2.5. Scheme of MDMA metabolism by wild-type (1) and Phe^{120}Ala mutant CYP2D6 into 3,4-OH-MA (1), MDA (2), and *N*-OH-MDMA (3) is shown in (B).

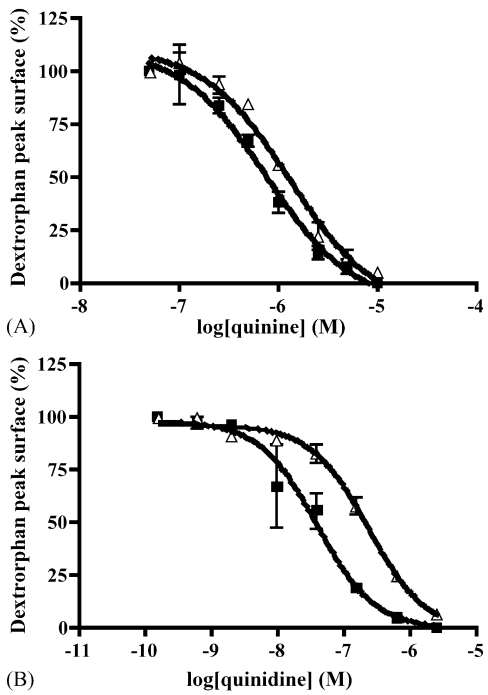

Fig. 3. Relative amounts of dextromethorphan *O*-demethylation in presence of various amounts of quinine (A) and quinidine (B) by Phe^{120}Ala mutant (Δ) and wild-type CYP2D6 (■). Plotted values are the means of at least two independent experiments ± S.D. as described in Section 2.5.

Table 2
IC_{50} values (μM) of the ligands quinine and quinidine against 8 μM dextromethorphan for wild-type and Phe^{120}Ala mutant CYP2D6

Ligand	Wild-type IC_{50} (μM)	Phe^{120}Ala IC_{50} (μM)
Quinidine	0.04 ± 0.01	0.24 ± 0.04
Quinine	0.76 ± 0.17	1.3 ± 0.27

All values are the means of at least two independent experiments ± S.D. as described in Section 2.5.

[12]. Furthermore, the constructed homology model used in this study has a more 'closed' binding pocket as a result of the fact that the substrate-free CYP2C5 crystal structure template used for the old homology model is lacking the F/G-loop (unpublished data).

4. Discussion

Recently computer homology modelling studies suggested Phe^{120} to be a CYP2D6 active site residue involved in the binding of substrates via aromatic interactions [9,11,12]. The primary aim of this study was to evaluate the role of this residue in the CYP2D6 active site. The results presented in this study show that Phe^{120} is very relevant in CYP2D6 ligand binding, substrate selectivity and regiospecificity in catalysis.

The expression levels of the Phe^{120}Ala mutant in *E. coli* were found to be lower than the wild-type enzyme, indicating that Phe^{120} may have a role in the stability of the enzyme. High levels of P420 were seen in the difference spectra, showing that the expression itself was not hampered, but that a large amount of enzyme formed was not functional as was reported before for several other CYP2D6 mutants [10,27].

Four typical CYP2D6 substrates were selected to characterise the Phe^{120}Ala mutant. Compared to wild-type CYP2D6, large substrate-dependent differences in metabolism were found after introducing a single mutation, not reported before for other CYP2D6 mutants. MAMC was not metabolised by the Phe^{120}Ala mutant while bufuralol metabolism by the Phe^{120}Ala mutant was similar to the metabolism by the wild-type enzyme. For both dextromethorphan and MDMA there were changes in regiospecificity after mutating Phe^{120} into an Ala. So, despite the fact that all four substrates show structural similarity in having a basic N-atom at about 7 Å of the site of oxidation and in having an adjacent aromatic moiety [14], still the influence of the mutation differed between these substrates. The only time large substrate-dependent differences were described for a CYP2D6 mutant was with a Glu^{216}Gln mutant, using the substrate spirosulfonamide [11] that lacks a basic N-atom and, therefore, does not fit into the classical pharmacophore model [14-16].

Neither HAMC nor other metabolites were detected after incubating MAMC with the Phe^{120}Ala mutant so apparently Phe^{120} influences either the affinity or the

orientation of this substrate with respect to the heme. More experiments with other coumarin derivatives could give more information about the underlying mechanisms [28].

Bufuralol metabolism by CYP2D6 was studied previously using a series of Asp^{301} mutants [24] and also mutants of Glu^{216} to non-acidic residues were studied using this model substrate [10,11]. Large effects were found on affinity and turnover of the mutants for this compound, showing that these acidic residues are more important for bufuralol metabolism than Phe^{120} as can be concluded from this study. The role of Asp^{301} was postulated also to be fixation of the B/C-loop containing residue Phe^{120} [10–12], however, the present results do not seem to support this role as the Phe^{120}Ala mutation hardly shows an effect on bufuralol metabolism. Consequently, the role of Asp^{301} does not seem to be merely the fixation of Phe^{120} into the active site [29], but creation of the net negative charge together with Glu^{216} may be of bigger importance.

N-Dealkylation of substrates is a possible route in CYP2D6 metabolism and Phe^{481} was predicted previously to be an important binding residue for these substrates [15]. However, mutating the Phe^{481} residue into a Gly did not have a large influence on *N*-deisopropylation of metoprolol [17]. Both MDMA and dextrorphan were *N*-demethylated by the Phe^{120}Ala mutant implicating a more promiscuous way of orientation of these two substrates in the active site of CYP2D6 and the involvement of the Phe^{120} residue in binding substrates undergoing *N*-dealkylation.

Besides *N*-dealkylation of MDMA, also *N*-hydroxylation occurred when MDMA was incubated with the Phe^{120}Ala mutant. *N*-OH-MDMA has been described before as a MDMA metabolite in horse urine [30]; however, from this study, it remained unclear what enzymes were playing a role in this reaction. Furthermore, aliphatic *N*-hydroxylation has not been described before as a metabolic reaction catalysed by CYP2D6 wild-type or mutants for any substrate. The co-occurrence of both *N*-dealkylation and *N*-hydroxylation of a single substrate has been reported once before for *N*-methylbenzamidine by rabbit CYP2C3 [31]. Additional work should give more insights in the mechanism of these transformations by the Phe^{120}Ala CYP2D6 mutant.

The role of Phe^{120} in the active site of CYP2D6 seems to be at least two-fold; firstly, the phenyl ring fills the active site cavity causing a reduction of its size, and secondly, it may have a function as an aromatic interaction site. The metabolite 3-hydroxymorphinan is detected exclusively in dextromethorphan incubations with the Phe^{120}Ala mutant. In Fig. 4, it is demonstrated how the mutation of the bulky Phe into a smaller Ala-residue allows the dextromethorphan *N*-demethylation binding mode to be accommodated more easily by creating more space in the CYP2D6 active site. As indicated earlier, Phe^{120} is considered important for interacting with quinidine via π-stacking [9]. The six-fold increase in IC_{50}-value as determined for the Phe^{120}Ala mutant validates the specific anchoring role of this residue.

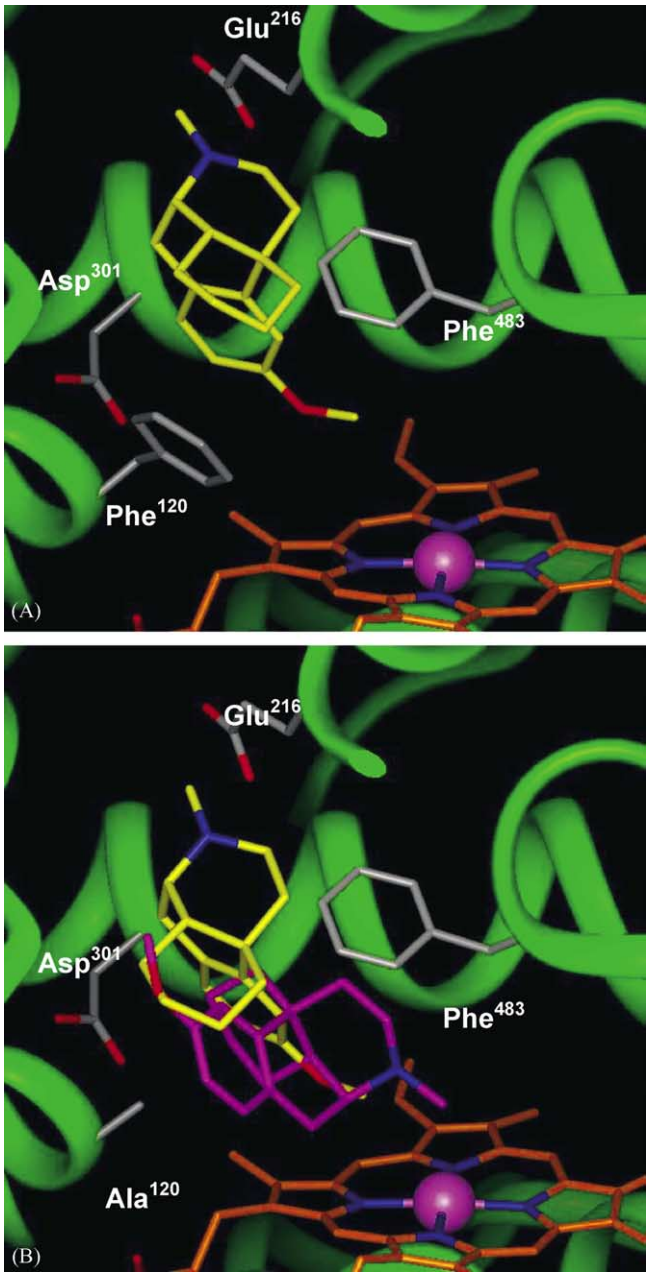

Fig. 4. Binding orientation of dextromethorphan automatically docked in the active site of the homology models of CYP2D6 using Autodock with standard conditions [32]. In wild-type CYP2D6, the orientation of dextromethorphan (in yellow) with its *O*-methyl pointing towards the heme is favoured (A), in the Phe^{120}Ala mutant two distinct orientations, supporting both *N*-demethylation (in magenta) as *O*-demethylation (in yellow) were found (B).

This role was confirmed by the inability of the Phe^{120}Ala mutant to metabolise MAMC. The two roles; space filling and aromatic anchoring, however, only partly explain the substrate specific influence, as bufuralol, MDMA and MAMC are structurally similar substrates but showed different changes in metabolism when incubated with the Phe^{120}Ala mutant.

In the rat isoforms of the CYP2D6 family, no homologous aromatic residues are present in the B/C-loop, so the

Phe^{120} is a human CYP2D6 active site-specific residue [9]. The data presented here introduce Phe^{120} as the fourth important residue in the binding of ligands to and catalysis by CYP2D6, next to Glu^{216}, Asp^{301} and Phe^{483}. The effects of removing the Phe^{120} phenyl-moiety are on the affinity, turnover and orientation of substrates, but the effects were quite different for structurally similar substrates. To rationalise the large differences found with the four chosen substrates, advanced molecular modelling is needed. Combined with molecular dynamics it can give insights where space is a limiting factor or where specific interactions play a role in the CYP2D6 active site.

Acknowledgements

We would like to thank Dr. Frans de Kanter for his help with recording and elucidating the NMR spectra and Ed Groot for his help in preparing the *E. coli* membranes.

References

[1] Estabrook RW. Cytochromes P450: from a single protein to a family of proteins with some personal reflections. In: Ioannides, Costas, editors. Cytochromes P450: metabolic and toxicological aspects. New York: CRC Press; 1996. p. 3–28.
[2] Goeptar AR, Scheerens H, Vermeulen NPE. Oxygen and xenobiotic reductase activities of cytochrome P450. Crit Rev Toxicol 1995;25:25–65.
[3] Zanger UM, Raimundo S, Eichelbaum M. Cytochrome P450 2D6: overview and update on pharmacology, genetics, biochemistry. Naunyn Schmiedebergs Arch Pharmacol 2004;369:23–37.
[4] Bertilsson L, Dahl ML, Dalen P, Al-Shurbaji A. Molecular genetics of CYP2D6: clinical relevance with focus on psychotropic drugs. Br J Clin Pharmacol 2002;53:111–22.
[5] Ingelman-Sundberg M, Oscarson M, McLellan RA. Polymorphic human cytochrome P450 enzymes: an opportunity for individualized drug treatment. Trends Pharmacol Sci 1999;20:342–9.
[6] Oscarson M. Pharmacogenetics of drug metabolising enzymes: importance for personalised medicine. Clin Chem Lab Med 2003;41: 573–80.
[7] Wester MR, Johnson EF, Marques-Soares C, Dansette PM, Mansuy D, Stout CD, et al. Structure of a substrate complex of mammalian cytochrome P450 2C5 at 2.3 Å resolution: evidence for multiple substrate binding modes. Biochemistry 2003;42:6370–9.
[8] Williams PA, Cosme J, Ward A, Angove HC, Matak Vinkovic D, Jhoti H, et al. Crystal structure of human cytochrome P4502C9 with bound warfarin. Nature 2003;424:464–8.
[9] Venhorst J, ter Laak AM, Commandeur JN, Funae Y, Hiroi T, Vermeulen NPE, et al. Homology modeling of rat and human cytochrome P450 2D (CYP2D) isoforms and computational rationalization of experimental ligand-binding specificities. J Med Chem 2003;46:74–86.
[10] Paine MJ, McLaughlin LA, Flanagan JU, Kemp CA, Sutcliffe MJ, Roberts GC, et al. Residues glutamate 216 and aspartate 301 are key determinants of substrate specificity and product regioselectivity in cytochrome P450 2D6. J Biol Chem 2003;278:4021–7.
[11] Guengerich FP, Hanna IH, Martin MV, Gillam EM. Role of glutamic acid 216 in cytochrome P450 2D6 substrate binding and catalysis. Biochemistry 2003;42:1245–53.
[12] Kirton SB, Kemp CA, Tomkinson NP, St-Gallay S, Sutcliffe MJ. Impact of incorporating the 2C5 crystal structure into comparative models of cytochrome P450 2D6. Proteins 2002;49:216–31.
[13] Smith G, Modi S, Pillai I, Lian LY, Sutcliffe MJ, Pritchard MP, et al. Determinants of the substrate specificity of human cytochrome P-450 CYP2D6: design and construction of a mutant with testosterone hydroxylase activity. Biochem J 1998;331:783–92.
[14] Koymans L, Vermeulen NPE, van Acker SA, te Koppele JM, Heykants JJ, Lavrijsen K, et al. A predictive model for substrates of cytochrome P450-debrisoquine (2D6). Chem Res Toxicol 1992; 5:211–9.
[15] de Groot MJ, Ackland MJ, Horne VA, Alex AA, Jones BC. A novel approach to predicting P450 mediated drug metabolism. CYP2D6 catalyzed *N*-dealkylation reactions and qualitative metabolite predictions using a combined protein and pharmacophore model for CYP2D6. J Med Chem 1999;42:4062–70.
[16] Vermeulen NPE. Prediction of drug metabolism: the case of cytochrome P450 2D6. Curr Top Med Chem 2003;3:1227–39.
[17] Hayhurst GP, Harlow J, Chowdry J, Gross E, Hilton E, Lennard MS, et al. Influence of phenylalanine-481 substitutions on the catalytic activity of cytochrome P450 2D6. Biochem J 2001;355:373–9.
[18] Onderwater RC, Venhorst J, Commandeur JN, Vermeulen NP. Design, synthesis, and characterization of 7-methoxy-4-(aminomethyl)coumarin as a novel and selective cytochrome P450 2D6 substrate suitable for high-throughput screening. Chem Res Toxicol 1999; 12:555–9.
[19] Braun U, Shulgin AT, Braun G. Centrally active *N*-substituted analogs of 3,4-methylenedioxyphenylisopropylamine (34-methylenedioxyamphetamine). J Pharm Sci 1980;69:192–5.
[20] de Boer D, Tan LP, Gorter P, van de Wal RM, Kettenes-van den Bosch JJ, de Bruijn EA, et al. Gas chromatographic–mass spectrometric assay for profiling the enantiomers of 3,4-methylenedioxymethamphetamine and its chiral metabolites using positive chemical ionization ion trap mass spectrometry. J Mass Spectrom 1997;32: 1236–46.
[21] Bauer S, Shiloach J. Maximal exponential growth rate and yield of *E. coli* obtainable in a bench-scale fermentor. Biotechnol Bioeng 1974;16:933–41.
[22] Omura T, Sato R. The carbon monoxide-binding pigment of liver microsomes. I. solubilization, purification, and properties. J Biol Chem 1964;239:2379–85.
[23] Venhorst J, Onderwater RC, Meerman JH, Vermeulen NPE, Commandeur JN. Evaluation of a novel high-throughput assay for cytochrome P450 2D6 using 7-methoxy-4-(aminomethyl)-coumarin. Eur J Pharm Sci 2000;12:151–8.
[24] Hanna IH, Krauser JA, Cai H, Kim MS, Guengerich FP. Diversity in mechanisms of substrate oxidation by cytochrome P450 2D6 lack of an allosteric role of NADPH-cytochrome P450 reductase in catalytic regioselectivity. J Biol Chem 2001;276:39553–61.
[25] Wester MR, Johnson EF, Marques-Soares C, Dijols S, Dansette PM, Mansuy D, et al. Structure of mammalian cytochrome P450 2C5 complexed with diclofenac at 2.1 Å resolution: evidence for an induced fit model of substrate binding. Biochemistry 2003;42: 9335–45.
[26] Lin LY, Di Stefano EW, Schmitz DA, Hsu L, Ellis SW, Lennard MS, et al. Oxidation of methamphetamine and methylenedioxymethamphetamine by CYP2D6. Drug Metab Dispos 1997;25: 1059–64.
[27] Hanna IH, Kim MS, Guengerich FP. Heterologous expression of cytochrome P4502D6 mutants, electron transfer, and catalysis of bufuralol hydroxylation: the role of aspartate 301 in structural integrity. Arch Biochem Biophys 2001;393:255–61.
[28] Venhorst J, Onderwater RC, Meerman JH, Commandeur JN, Vermeulen NPE. Influence of *N*-substitution of 7-methoxy-4-(aminomethyl)-coumarin on cytochrome P450 metabolism and selectivity. Drug Metab Dispos 2000;28:1524–32.

[29] Guengerich FP, Miller GP, Hanna IH, Martin MV, Leger S, Black C, et al. Diversity in the oxidation of substrates by cytochrome P450 2D6: lack of an obligatory role of aspartate 301-substrate electrostatic bonding. Biochemistry 2002;41:11025–34.

[30] Dumasia MC. Identification of some *N*-hydroxylated metabolites of (+/−)-3,4-methylenedioxymethamphetamine in horse urine by gas chromatography–mass spectrometry. Xenobiotica 2003;33:1013–25.

[31] Clement B, Jung F. *N*-hydroxylation and *N*-dealkylation by CYP2C3 of *N*-methylbenzamidine: *N*-oxygenation and *N*-oxidative dealkylation of one functional group. Xenobiotica 1995;25:443–55.

[32] Morris GM, Goodsell DS, Halliday RS, Huey R, Hart WE, Belew RK, et al. Automated docking using a Lamarckian genetic algorithm and an empirical binding free energy function. J Comput Chem 1998; 19:1639–62.